Lattice dynamics of high-T_c superconductors: Optical modes of the thallium-based compounds

A. D. Kulkarni and F. W. de Wette

Department of Physics, University of Texas, Austin, Texas 78712-1081

J. Prade and U. Schröder

Universität Regensburg, D-8400 Regensburg, Federal Republic of Germany

W. Kress

Max-Planck-Institut für Festkörperforschung, Postfach 80 06 65, D-7000 Stuttgart 80, Federal Republic of Germany

We present a lattice-dynamical calculation of the Raman- and infrared-active modes of the following six thallium-based high-T_c superconductors: $Tl_2Ba_2CuO_6$, $Tl_2CaBa_2Cu_2O_8$, and $Tl_2Ca_2Ba_2Cu_3O_{10}$ (body-centered-tetragonal structures) and $TlCaBa_2Cu_2O_7$, $TlCa_2Ba_2Cu_3O_9$, and $TlCa_3Ba_2Cu_4O_{11}$ (simple-tetragonal structures). Our calculations are based on a shell model that incorporates short-range overlap potentials, long-range Coulomb potentials, and ionic polarizabilities. We also require that the shell models for different high-T_c superconducting compounds be mutually compatible, namely that the short-range potentials for given ion pairs in equivalent environments be transferable from one compound to the other. The model presented here does in fact utilize a common set of short-range potentials that apply to the entire series of thallium-based superconductors as well as to $YBa_2Cu_3O_7$ and $Bi_2CaSr_2Cu_2O_8$, studied earlier. The model reproduces the available experimental infrared and Raman data of all these compounds quite well and is thus supported by a broad database, albeit only of optical modes. We expect that our model, which is based on realistic interaction potentials, reproduces eigenvalues and eigenvectors to the same approximation. Thus we conclude from the satisfactory agreement between calculated and measured eigenfrequencies that the calculated eigenvectors provide a realistic description of the displacement patterns of the optical modes.

I. INTRODUCTION

Recently we calculated the Raman- and infrared-active modes of $Tl_2CaBa_2Cu_2O_8$.[1] These calculations were carried out with a lattice-dynamical interaction model which leads to stable phonon dynamics in the whole Brillouin zone for $YB_2Cu_3O_7$,[2] $Bi_2CaSr_2Cu_2O_8$,[3] as well as for the six thallium-based compounds discussed here (cf. next section), and reproduces the experimental optical data of these materials rather well. Our approach[2-4] is based on the use of long-range Coulomb potentials and short-range repulsive Born-Mayer potentials, in the framework of a shell model. The justification and advantages of using short-range *potentials* instead of force constants in the lattice dynamics of the high-T_c superconductors are:[1] First, these compounds are predominantly ionic-type materials. Because of the closed-shell electronic configurations, the short-range interactions of ion pairs can be represented by Born-Mayer potentials that are largely independent of the spatial arrangement and the crystal surrounding of the interacting ion pair. Hence these potentials are to a good approximation transferable from one compound to another. Second, if force constants were to be used, only a relatively small number of experimental phonon frequencies would be available to determine the large number of force constants needed

(because of the large number of particles in the unit cell). This would leave a large amount of arbitrariness in the choice of these force constants, which in turn would lead to a poorly defined model, whose predictions for the phonon eigenvectors would be quite unreliable.

In the implementation of this scheme for the Tl-based compounds we transferred the Cu-O, O-O and Ba-O potentials directly from our model for $YBa_2Cu_3O_7$,[2] and the Ca-O potential from our model for $Bi_2CaSr_2Cu_2O_8$.[3] The Tl-O interaction poses a special problem because of its anisotropy, manifested in the fact that in the Tl-based structure the *interplanar* Tl-O distance is significantly smaller than the *intraplanar* Tl-O distance. As a consequence, in order to obtain stable phonon dynamics, we had to introduce different sets of Born-Mayer potentials for interplanar and intraplanar interactions (cf. Ref. 1). Finally, we required that a set of common Born-Mayer potentials lead to stable phonon dynamics for *all* the compounds mentioned above.[5] This turned out to be a very stringent requirement on the model, which significantly restricted the range of adjustments in parameter space. On the other hand, the fact that we were able to develop a unified set of potentials for these eight compounds is a confirmation of the validity of our approach to the lattice dynamics of these materials.

We should comment here on the extent to which we

have attempted to obtain agreement with the experimental optical data presently available, which is extremely limited, even if taken together for all the compounds. From the point of view of a lattice-dynamical description, there may (and almost certainly will) exist a variety of complications in the ionic interactions in these compounds, such as noncentral contributions (many-body forces), hybridization of electronic states (charge transfer), anharmonicities, etc., which are not contained in our model so far. The effects of such interactions might possibly be exhibited by inelastic neutron scattering measurements of the phonon dispersion curves over the entire Brillouin zone. Such additional information will probably call for further adjustments in the short-range potentials, and possibly require the inclusion of electronic excitations other than those of dipolar symmetry which are already included in the model. Therefore, in the absence of more complete information, it is not useful to attempt to match the available experimental information too closely. (Incidentally, this consideration also puts in perspective the limited usefulness of approaches that are restricted to reproducing just the measured optical modes, such as is done in the normal coordinate analysis.) In view of this we have used the measured Raman A_{1g} frequencies for only one compound, namely, $Tl_2CaBa_2Cu_2O_8$, to determine the Tl-O interaction parameters which could not be directly taken over from our previous work (cf. Ref. 1).

II. CALCULATIONS

A. Structures

We have performed calculations for the following compounds: $Tl_2Ba_2CuO_6$ (2:0:2:1:6), $Tl_2CaBa_2Cu_2O_8$ (2:1:2:2:8),[1] $Tl_2Ca_2Ba_2Cu_3O_{10}$ (2:2:2:3:10), all of which have body-centered-tetragonal (bct) structures (space group $I4/mmm$), and $TlCaBa_2Cu_2O_7$ (1:1:2:2:7), $TlCa_2Ba_2Cu_3O_9$ (1:2:2:3:9), $TlCa_3Ba_2Cu_4O_{11}$ (1:3:2:4:11), all of which have simple tetragonal (st) structures (space group $P4/mmm$). The structural data for the bct structures 2:0:2:1:6, 2:1:2:2:8, and 2:2:2:3:10 were taken from Shimakawa et al.[6] For the st structures 1:1:2:2:7 and 1:2:2:3:9 the structural data were taken from Morosin et al.,[7,8] respectively. The structural data for 1:3:2:4:11 were unavailable and hence were derived by extrapolating those for 1:2:2:3:9.[8] The structure of 1:3:2:4:11 thus obtained agrees very well with the results of high-resolution transmission electron microscope measurements of Ihara et al.[9]

The polarization data will be pictorially presented in rectangular cells, which are the primitive cells for the st structures (1:1:2:2:7, 1:2:2:3:9, 1:3:2:4:11) but not for the bct structures (2:0:2:1:6, 2:1:2:2:8, 2:2:2:3:10; cf. Fig. 1). The advantage of this kind of presentation (in which the pairs 1:1:2:2:7/2:1:2:2:8, and 1:2:2:3:9/2:2:2:3:10 are represented by the same diagrams) is that the common features of the modes of a given symmetry in the successive structures are brought out most clearly. However, the following should be noted. It may appear from the diagrams that the thallium-oxygen planes are mirror

planes of these structures. While this is so for the st structures, it is not so for the bct structures. As a consequence the ions in Tl-O planes have to remain stationary in all Raman modes of the st structures, but not necessarily in those of the bct structures. Finally, the nomenclature of the Cu and O ions in the various structures is also indicated in Fig. 1.

B. Model

As was mentioned in the Introduction the shell model used in these calculations has a unique set of short-range interaction potentials for the various ionic interactions, and one set of ionic polarizabilities, which are common to all compounds treated here. The model parameters are given in Table I. Note that we have used different values for the ionic charge of Tl in the bct and st structures. This was necessary to obtain stable phonon dynamics for all six compounds. It can be verified that with the use of charge neutrality of the chemical unit of each compound, the nominal ionic charge of Tl turns out to be 3+ and 4+ for the bct and st structures, respectively. Thus our use of a larger ionic charge for Tl in the st structures as compared to that in the bct structures is consistent with this observation. With the use of the ionic charges listed in Table I, the ionic charge of oxygen is determined by charge neutrality of each compound. It is approximately 1.9− for all six compounds; the exact values are given in footnote h of Table I.

In our previous work[1-4] we specified the on-site core-shell force constants k in units e^2/v_a where e is the electronic charge and v_a is the volume of the primitive cell of the compound under consideration. This representation is inconvenient in the present case since the value of v_a varies from one compound to the next. Hence in Table I we report the free ion polarizabilities $\alpha_i = Y_i^2/k_i$ for each ion i, where Y_i is the shell charge and k_i is the on-site core-shell force constant expressed in units $e^2/\text{Å}^3$. Specifying α instead of k (in units e^2/v_a) also makes it trans-
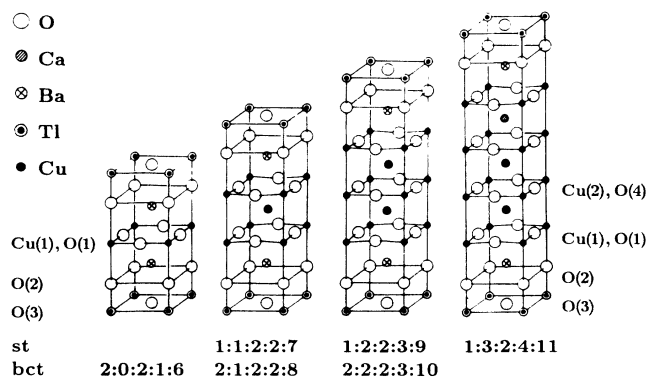
FIG. 1. Rectangular cells for the six thallium compounds; they are primitive cells for the st structures but not for the bct structures. The Cu(1), O(1) planes are the Cu-O planes adjacent to the Ba-O(2) planes. All other Cu-O planes are Cu(2), O(4). Note that 2:0:2:1:6, 1:1:2:2:7, and 2:1:2:2:8 have no Cu(2), O(4) planes, 1:2:2:3:9 and 2:2:2:3:10 have one, and 1:3:2:4:11 has two.

TABLE I. Parameters of the model: a, b: Born-Mayer constants; Z, Y, α: ionic charge, shell charge, and polarizability of the ion.

Interaction	a (eV)	$b(\text{Å}^{-1})$	Ion	$Z(|e|)$	$Y(|e|)$	$\alpha(\text{Å}^3)$
Tl-O[a]	3000	2.80	Tl[c]	2.70	2.00	0.8687
Tl-O[b]	3000	3.55	Tl[d]	3.00	2.00	0.8687
Ba-O	3225	2.90	Ba	2.00	2.32	5.6472
Ca-O	2513	3.10	Ca	2.00	0.50−	0.0400
Cu-O	1260	3.35	Cu	2.00	3.22	1.7972
O-O	1000	3.00	O[e]	h	2.70−	5.0103
			O[f]	h	2.70−	0.7539
			O[g]	h	2.70−	5.0103 ($\alpha_\parallel$)
						0.7539 ($\alpha_\perp$)

[a]For Tl and O in the same plane (intraplanar interaction).
[b]For Tl and O in adjacent planes (interplanar interaction).
[c]For Tl in 2:0:2:1:6, 2:1:2:2:8, and 2:2:2:3:10 (bct structures).
[d]For Tl in 1:1:2:2:7, 1:2:2:3:9, and 1:3:2:4:11 (st structures).
[e]For O in the Cu-O planes.
[f]For O in the Tl-O planes.
[g]For O in the Ba-O planes. For the O in these planes we assume anisotropic polarizability with $\alpha_\parallel$ parallel to the Cu-O-Tl directions and $\alpha_\perp$ perpendicular to those directions.
[h]The ionic charge of O is determined by charge neutrality of the chemical unit. It is 1.90−, 1.93−, 1.94−, for 2:0:2:1:6, 2:1:2:2:8, 2:2:2:3:10, respectively, and 1.86−, 1.89−, 1.91−, for 1:1:2:2:7, 1:2:2:3:9, 1:3:2:4:11, respectively.

parent that the same values of α are used for all six compounds.

III. RESULTS

The calculated mode frequencies for the Raman modes (A_{1g}, B_{1g}, E_g) and infrared (ir) modes (A_{2u}, B_{2u}, E_u), for the six structures, are presented in Tables II through V. For the purpose of comparison we have included the results for 2:1:2:2:8, which have been published earlier.[1] The column headings list the abbreviations of the structures, with the last number indicating the number of oxygen ions in the unit cell. "Similar" modes, i.e., modes in

TABLE II. Vibrational characteristics and comparison of the calculated and measured A_{1g} and B_{1g} (Raman) modes. The mode frequencies are expressed in cm^{-1}. The available experimental data are given in parentheses and the corresponding references appear in the column headings. A prime (in the fifth column) denotes a 180°-out-of-phase-vibration; e.g., O(1), O(4), Ca' indicates that O(1) and O(4) vibrate in phase and Ca vibrates 180° out of phase of O(1) and O(4).

	2:0:2:1:6 Ref. 13	1:1:2:2:7 Ref. 14	2:1:2:2:8 Refs. 16 and 17		1:2:2:3:9 Ref. 17	2:2:2:3:10 Ref. 17	1:3:2:4:11
			A_{1g} modes				
Ba	129 (125)	123 (120)	119 (108)	Ba, Cu(1), Cu(2)[a]	113 (104)	104[b] (99)	101
Tl	153 (165)	—	138 (130)	Tl', Ba, Cu(1)	—	126 (133)	—
Cu(1)	—	137 (148)	149 (158)	Cu(1), Ba', Cu(2)[a]	131 (152)	144 (159)	127
	—	—	—	Cu(1), Cu(2)'	—	—	142
O(1)	—	358	370 (407)	O(1), O(4)[a], Ca	293 (260)	302 (270)	246
	—	—	—	O(4), O(1)'	—	—	369
	—	—	—	O(1), O(4)[a], Ca'	449	456 (407)[c]	450
O(2)	445 (485)	494 (525)	439 (494)		505 (526)	420 (498)	503
O(3)	640 (603)	—	623 (599)		—	608 (601)	—
			B_{1g} modes				
O(1)	—	296 (278)	303	O(1), O(4)[a]	260 (238)	256 (245)[c]	206
	—	—	—	O(1), O(4)'	—	—	298

[a]Cu(2) and O(4) ions vibrate only in 1:3:2:4:11 [and not in 1:2:2:3:9 and 2:2:2:3:10 since the Cu(2)-O(4) plane is a mirror plane in 1:2:2:3:9 and 2:2:2:3:10; cf. Fig. 1].
[b]In this mode Tl ions also vibrate in addition to Ba and Cu(1).
[c]K. F. McCarty, private communication.

TABLE III. Vibrational characteristics of the calculated E_g (Raman) modes. The mode frequencies are expressed in cm^{-1}. The notation Cu(1) plane (in column 1) denotes that *all* the ions [Cu(1) and O(1)] in the Cu(1)-O(1) plane participate in phase in the vibration. A prime (in the fifth column) denotes a 180° out-of-phase vibration; e.g., O(1), O(4), Ca' indicates that O(1) and O(4) vibrate in phase and Ca vibrates 180° out of phase of O(1) and O(4).

	2:0:2:1:6	1:1:2:2:7	2:1:2:2:8		1:2:2:3:9	2:2:2:3:10	1:3:2:4:11
Ba	100	80.6	75.9	Ba,Cu(1) planes; Ca	71.6	66.5	64.8
Tl	131	—	136		—	136	—
Cu(1) plane	—	138	147	Cu(1) plane; Ba', Ca	129	140	107[a]
	—	—	—	Cu(1), Cu(2)' planes	—	—	135
	—	—	—	O(1), O(4)[b] angle bends; Ca	251	259	251
	—	—	—	O(4), O(1)' angle bends	—	—	352
O(1) angle bend	—	338	350	O(1), O(4)[b] angle bends; Ca'	381	375	385
O(2)	388	396	401		397	415	399
O(3)	491	—	493		—	489	—
O(1) stretch	—	565	557		561	555	558
	—	—	—	O(4) stretch	—	—	561

[a]In this mode the Cu(2) plane vibrates instead of the Cu(1) plane.
[b]Cu(2) and O(4) ions vibrate only in 1:3:2:4:11 [and not in 1:2:2:3:9 and 2:2:2:3:10 since the Cu(2)-O(4) plane is a mirror plane in 1:2:2:3:9 and 2:2:2:3:10; cf. Fig. 1].

TABLE IV. Vibrational characteristics of the calculated A_{2u} and B_{2u} (ir) modes. The mode frequencies are expressed in cm^{-1}. The numbers in parentheses are frequencies of the longitudinal optical (LO) modes. The corresponding transverse optical (TO) frequencies are given above the LO frequencies. A prime denotes a 180°-out-of-phase-vibration; e.g., Cu(1), Ba, Tl' indicates that Cu(1) and Ba vibrate in phase and Tl vibrates 180° out of phase of Cu(1) and Ba.

	2:0:2:1:6	1:1:2:2:7	2:1:2:2:8		1:2:2:3:9	2:2:2:3:10	1:3:2:4:11
			A_{2u} modes				
Cu(1)	—	77.6 (103)	—	Cu(1), Cu(2)	78.0 (97.0)	72.8 (103)	78.7 (93.5)
Cu(1), Ba, Tl'	108 (108)	—	108 (108)	Cu(2), Cu(1), Tl'	—	104 (131)	—
Cu(1), Ba'	129 (143)	—	113 (134)		—	—	—
Tl, Ba'	—	125 (134)	—		129 (134)	—	129 (131)
	—	—	—	Cu(2), Cu(1)'	139 (142)	150 (151)	132 (139)
O(1), Ca	294[a] (341)[a]	207 (224)	210 (238)	O(4), O(1), Ca	176 (188)	175 (197)	160 (167)
O(2), Ca'	—	349 (433)	355 (437)	O(2), Ca', O(1)	333 (364)	292 (372)	295 (323)
	—	—	—	O(4), O(2), Ca'	373 (438)	383 (421)	352 (432)
	—	—	—	Ca, O(2), O(4)'	—	—	432 (437)
O(2), O(1)', Ca	413[a] (451)[a]	445 (449)	457 (462)		445 (447)	443 (454)	446 (450)
O(3)	602 (648)	546 (566)	591 (630)		556 (572)	583 (616)	560 (574)
			B_{2u} modes				
O(1)	259	189	159	O(4), O(1)	155	133	116
	—	—	—	O(4), O(1)'	303	306	281

[a]There is no Ca vibration in this mode since 2:0:2:1:6 does not contain any Ca.

TABLE V. Vibrational characteristics of the calculated E_u (ir) modes. The mode frequencies are expressed in cm^{-1}. See the captions of Tables III and IV for explanation of the notation.

	2:0:2:1:6	1:1:2:2:7	2:1:2:2:8		1:2:2:3:9	2:2:2:3:10	1:3:2:4:11
Tl', Cu(1) planes; Ca, Ba	84.3[a] (86.0)[a]	97.3 (97.7)	79.5 (80.6)	Cu(2),Tl' planes; Ca	78.6 (78.9)	70.1 (70.7)	64.5 (64.5)
Ca, Ba'; Cu(1) plane	—	124 (124)	128 (128)	Tl, Cu(2) planes; Ba'	109 (109)	101 (101)	107[b] (107)[b]
Cu(1) plane; Ba'	162 (163)	—	—	Cu(1), Cu(2)' planes; Ba'	135 (135)	145 (145)	132 (133)
Ca; O(1) angle bend	—	240 (240)	254 (254)	Ca; O(4), O(1) angle bends	245 (245)	255 (255)	247 (247)
	—	—	—	Ca'; O(1) angle bend	—	—	255 (255)
O(1) angle bend	320 (326)	—	—	O(4), O(1)' angle bends	351 (351)	359 (359)	365 (372)
O(2), O(3)	381 (419)	359 (375)	393 (432)		358 (372)	401 (446)	356 (361)
Ca'; O(1) angle bend	—	382 (419)	382 (392)	Ca'; O(1), O(4) angle bends	392 (433)	387 (397)	389 (434)
O(3), O(2)'	425 (451)	448 (448)	444 (456)		451 (451)	451 (456)	453 (453)
O(1) stretch	559 (563)	567 (570)	558 (563)		560 (562)	555 (556)	558 (559)
	—	—	—	O(4) stretch	565 (568)	558 (563)	562 (566)

[a]There is no Ca vibration in this mode since 2:0:2:1:6 does not contain any Ca.
[b]In this mode the Cu(1) plane vibrates instead of the Cu(2) plane.

which similar sets of particles vibrate, are arranged in the rows, labeled by the ions carrying out the predominant vibrations (cf. Fig. 1). A prime denotes a 180° out-of-phase vibration of the ion. For the Raman A_{1g} modes the available experimental frequencies are indicated in parentheses, with the number of the reference appearing under the compound symbol. For the ir modes (Tables IV and V) the number in parentheses is the longitudinal frequency. A bar instead of an entry indicates that the mode does not occur in the compound. For instance, in the st structures 1:1:2:2:7, 1:2:2:3:9, and 1:3:2:4:11, the Tl-O(3) plane is a mirror plane (cf. Fig. 1) so that the ions in this plane must remain stationary in the Raman modes, as a result of symmetry. Thus the Raman modes in which Tl or O(3) vibrate do not occur in these compounds (see Tables II and III). Space limitations prevent us from publishing the complete sets of polarization diagrams for all of these compounds. However, as a representative example we display the complete set for 2:2:2:3:10 in Figs. 2 and 3. Moreover, the complete set for 2:1:2:2:8 has already been given in Ref. 1. (The A_{1g} modes of 1:1:2:2:7 will be presented in Ref. 10.) These two complete sets of diagrams, together with some specific examples given below (Figs. 4, 5, and 6), are sufficient to illustrate and discuss the systematics and the overall trends in the comparison of equivalent modes in the various compounds.

We begin by commenting on the frequency change of equivalent modes, in going from the smallest (2:0:2:1:6) to the largest (1:3:2:4:11) structure. This is the effect of inserting additional Ca ions and Cu-O layers (abbreviated as Ca/Cu-O units). In the tables this corresponds to following the frequencies in a given row from left to right. We point to the following overall trends.

(a) If there exists a variation in frequency going across a row ("similar" modes), the frequency usually diminishes from left to right, i.e., from the smaller to the larger unit. This is a mass effect because usually the cluster of particles involved in the vibration becomes larger, and therefore the reduced mass associated with that particular mode also becomes larger.

(b) This diminishing in frequency can occur along an entire row (cf. first row in Table II), but it is even more evident in the bct (2:0:2:1:6, 2:1:2:2:8, 2:2:2:3:10) and st (1:1:2:2:7, 1:2:2:3:9, 1:3:2:4:11) sequences, separately (cf. first row in Table V). Moreover, the decline in frequency may occur in one sequence, but not in the other [cf. eighth row (O(2) vibrations) in Table II]. This must be a subtle effect due to the difference in symmetry.

(c) In general the frequency variations for "similar" modes are much smaller for the xy-polarized modes (Tables III and V) than for the z-polarized modes (Tables II and IV). The reason is that the insertion of an additional Ca ion and a Cu-O layer (Ca/Cu-O unit) affects these vibrations only through the transverse force constants which are generally an order of magnitude smaller than the radial force constants; the latter come into play for the z-polarized modes when an addtional Ca/Cu-O

Raman A₁ₑ **Raman B₁ₑ**

104 126 144 302 420 456 608 256

Raman Eₑ

66.5 136 140 259 375 415 489 555
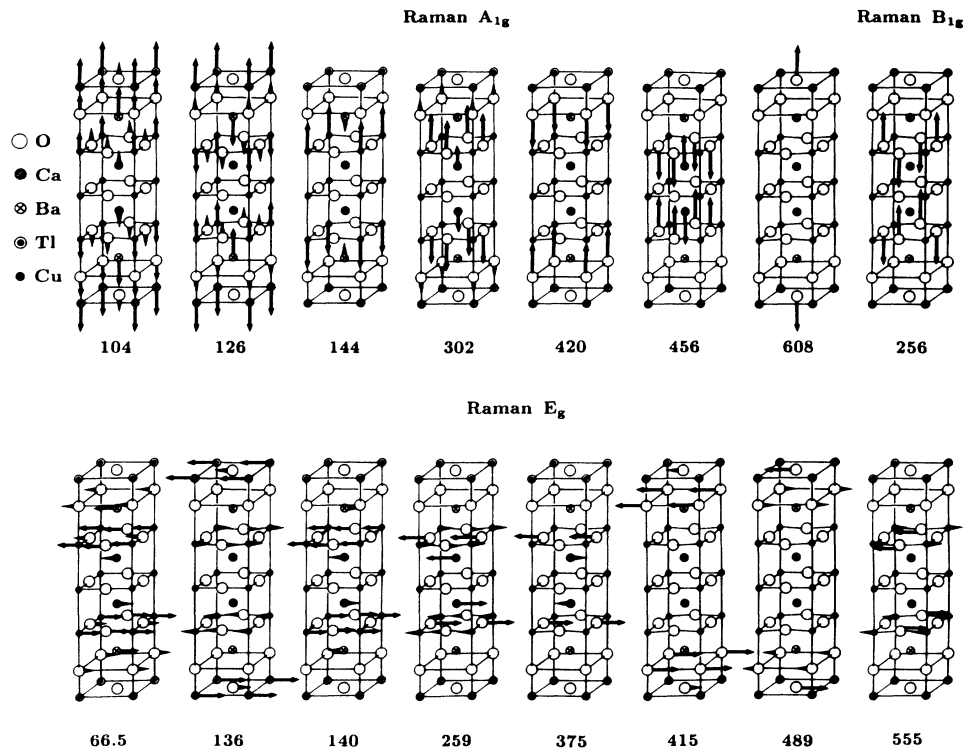
FIG. 2. Polarization diagrams of Raman modes of $Tl_2Ca_2Ba_2Cu_3O_{10}$. The mode frequencies are expressed in cm^{-1}. Long, medium, and short arrows indicate large, intermediate, and small amplitudes, respectively (amplitudes not to scale).

unit is inserted. This is particularly evident for the higher-frequency A_{2u}, B_{2u} modes (Table IV), and E_u modes (Table V).

(d) Among the six compounds, only 1:3:2:4:11 has two

pairs of inequivalent Cu-O planes, namely, Cu(1)-O(1) and Cu(2)-O(4) (cf. Fig. 1). As a consequence this compound has two B_{1g} modes (Table II) in which O(1) and O(4) vibrate in phase and 180° out of phase, respectively (cf. Fig.

Infrared A₂ᵤ TO (LO) **Silent Modes B₂ᵤ**

72.8 (103) 104 (131) 150 (151) 175 (197) 292 (372) 383 (421) 443 (454) 583 (616) 133 306

Infrared Eᵤ TO (LO)

70.1 (70.7) 101 (101) 145 (145) 255 (255) 359 (359) 387 (397) 401 (446) 451 (456) 555 (556) 558 (563)
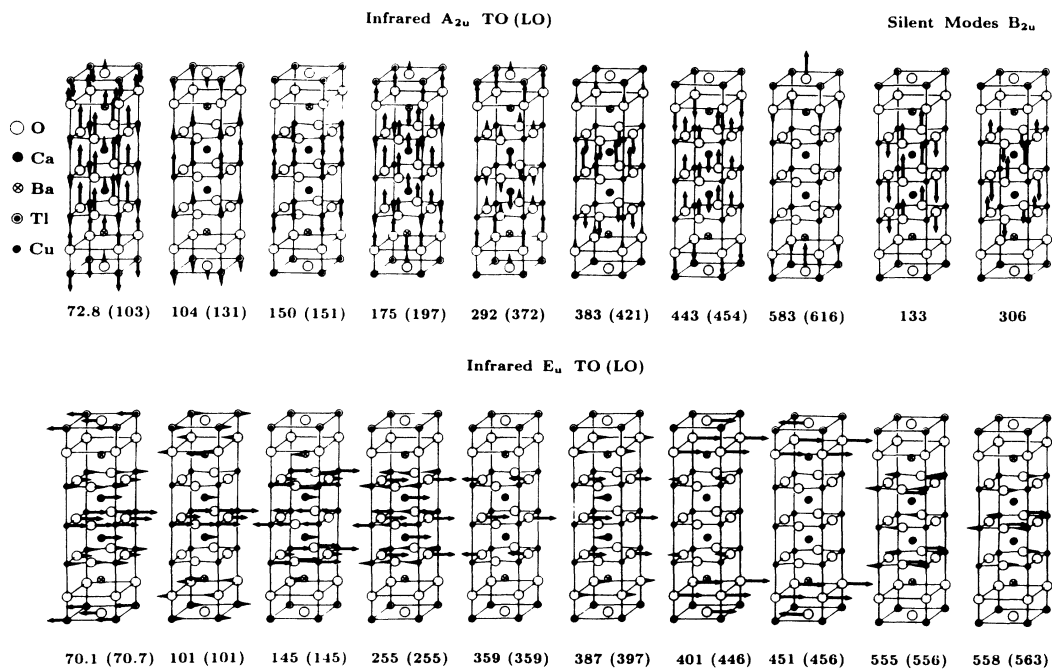
FIG. 3. Polarization diagrams of ir modes of $Tl_2Ca_2Ba_2Cu_3O_{10}$. The mode frequencies are expressed in cm^{-1}. The numbers in parentheses are LO frequencies which are preceded by their TO counterparts. Long, medium, and short arrows indicate large, intermediate, and small amplitudes, respectively (amplitudes not to scale).

Raman A_{1g} Modes

1:2:2:3/2:2:2:3   1:2:2:3/2:2:2:3

1:1:2:2/2:1:2:2

293/302   358/370   449/456

1:3:2:4

246   369   450
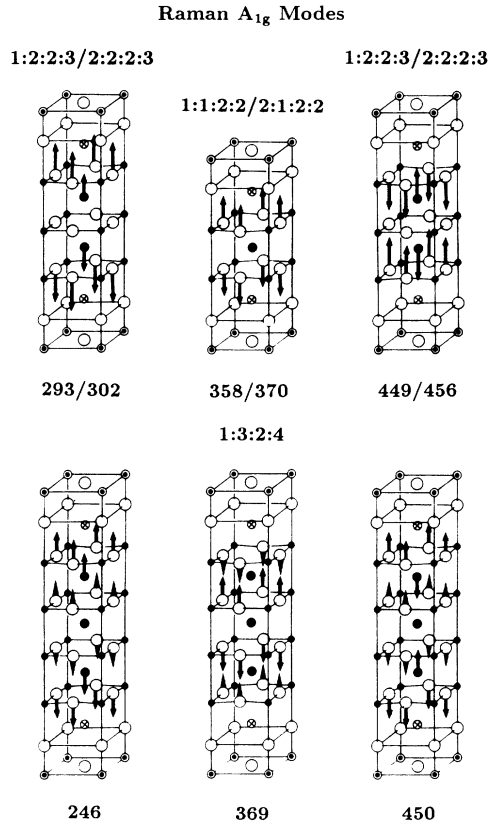
FIG. 4. Illustration of the effect of the insertion of additional Ca/Cu-O units on the frequencies and polarizations of certain Raman A_{1g} modes. The frequencies are expressed in cm^{-1}.

Raman B_{1g} Modes

1:1:2:2/2:1:2:2   1:2:2:3/2:2:2:3

296/303   260/256

1:3:2:4

206   298

FIG. 5. Comparison of the frequencies (in cm^{-1}) and polarizations of the Raman B_{1g} modes.

5). This difference accounts for the difference in frequency of these modes (206 and 298 cm^{-1}, respectively). A similar situation exists for the B_{2u} modes of 1:3:2:4:11 (Table IV). The energy difference of this pair (116 and 281 cm^{-1}) is even larger because for the 116-cm^{-1} mode the O in all Cu-O planes vibrate in phase.

(e) We illustrate the effect of the insertion of additional Ca/Cu-O units on the Raman A_{1g} modes in Fig. 4. In the 1:1:2:2:7/2:1:2:2:8 cell the Ca ion must remain stationary since it is located at the center of inversion (of both structures). In the 1:2:2:3:9/2:2:2:3:10 cell the addition of a Ca/Cu-O unit results in a Cu(2)-O(4) plane whose atoms are located at centers of inversion, and therefore the Cu(2)-O(4) plane remains stationary in the A_{1g} modes. In the Ca/Cu-O units above and below this plane, the Ca ion can vibrate in phase with the neighboring nonstationary Cu(1)-O(1) plane, leading to lower frequencies (left diagram), or 180° out of phase, leading to higher frequencies (right diagram). Similar arguments account for the differences in the frequencies in the 1:3:2:4:11 diagrams below.

It is generally believed that the superconductivity takes place in the Cu-O planes. Therefore, if any phonons are involved in the underlying mechanism of the superconductivity, they most probably involve displacements in the Cu-O planes. We therefore discuss the relevant

modes in more detail. Up to now the main evidence for a connection between superconductivity and lattice vibrations is found for the Raman B_{1g} modes, in which pairs of opposite oxygen ions in a Cu-O plane vibrate 180° out of phase (last two rows of Table II; Fig. 5): It has been found for $YBa_2Cu_3O_7$ that this mode has a slightly lower frequency in the superconducting phase than in the normal phase.[11] As is seen from Fig. 5, in the compounds that share the same polarization pattern (the pairs 1:1:2:2:7/2:1:2:2:8 and 1:2:2:3:9/2:2:2:3:10), the B_{1g} modes have virtually the same frequency; the frequency diminishes as one goes through the series from the simple to the more complex compounds. In 1:2:2:3:9/2:2:2:3:10, as compared to 1:1:2:2:7/2:1:2:2:8, the vibrating oxygen ions are separated by the stationary Cu-O plane, hence the frequency is somewhat lower, as expected. The B_{2u} modes (last two rows in Table IV) are the Davydov partners of the B_{1g} modes; these modes are silent because the dipole moment of the unit cell does not vary during motion. Since the central plane of the cell is not a mirror plane for these modes (as it is for the B_{1g} modes, cf. Fig.

IR A_{2u} Modes
Large TO–LO Splitting

2:0:2:1   1:1:2:2   2:1:2:2

294(341)   349(433)   355(437)

1:2:2:3   2:2:2:3   1:3:2:4

373(438)   292(372)   352(432)
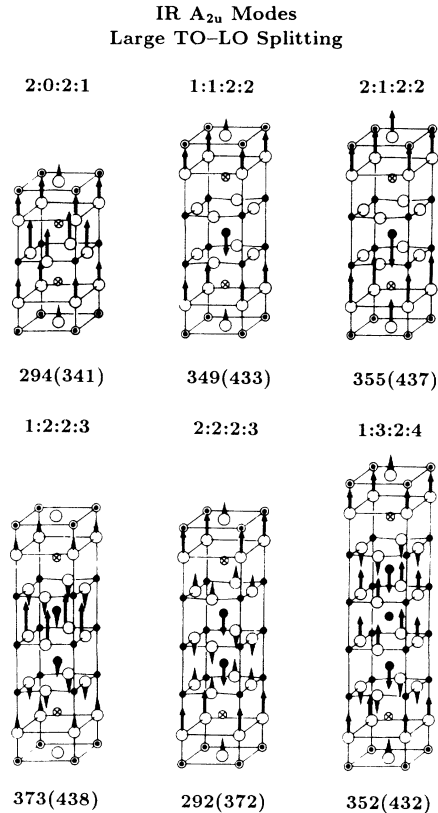
FIG. 6. Frequencies (in cm^{-1}) and polarizations of the ir A_{2u} modes with the largest TO-LO splittings. The frequencies in parentheses are the LO frequencies and are preceded by their TO counterparts.

5), a B_{2u} mode also appears in 2:0:2:1:6. Remarks about frequency comparisons for these modes were made under point (d).

Generally the same comments as were made for the B_{1g} modes, apply for those A_{1g} modes in which the oxygen ions in the same Cu-O plane all vibrate in phase [cf. fifth row (O(1) vibrations) in Table II; Fig. 4]. However, the frequencies are somewhat higher in the A_{1g} modes than in the B_{1g} modes since in the A_{1g} modes all O ions in the same plane vibrate in phase, and 180° out of phase with the neighboring planes, while the B_{1g} modes neighboring atoms in the same Cu-O plane vibrate out of phase with each other, in addition to vibrating out of phase with O ions in neighboring planes.

Finally, if one considers the vibrations of the oxygen and copper ions within the Cu-O planes (xy vibrations), i.e., the E_g and E_u modes (Tables III and V, respectively), one finds for a given mode hardly any change in frequency in going through the series. As noted above, this is due to the fact that for these modes the interactions between planes are governed by the transverse force constants so that inserting additional Ca/Cu-O units has little effect on the frequencies. Comparing the frequencies of the various E_g and E_u modes one can again, in broad terms, account for their differences by considering the relative vibrational phases of neighboring ions.

Summarizing this brief overview, one can say that in qualitative terms the overall dynamics of the optical modes is quite understandable on the basis of the interaction models, and does not contain any unusual features.

A. TO-LO splitting

The TO-LO splitting of the infrared-active modes results from the dynamic dipole moment associated with these modes. The A_{2u} modes with a large TO-LO splitting should show up prominently in infrared absorption experiments on these materials (cf. Ref. 12) whereas due to the presence of free carriers in the xy planes, the E_u modes would be difficult to observe. In Fig. 6 we show the displacement patterns of the ir-active A_{2u} modes with the largest TO-LO splittings (also see Table IV). The common feature of these modes is that they all predominantly involve oxygen vibrations: Cu-O-plane oxygen vibrations in four cases, O(2) vibrations in all cases, and O(3) vibrations in all but one (1:2:2:3:9). All these modes lie between 290 and 380 cm^{-1}. A comparison of the ir-active modes of 2:1:2:2:8 observed by Zetterer et al.[12] with our calculations has already been given in our previous work (Table II in Ref. 1) and hence will not be repeated here.

Most of the E_u modes show hardly any TO-LO splitting. Those with the largest TO-LO splittings (rows 7 and 8 of Table V) are also restricted mainly to oxygen vibrations, but they show a more systematic pattern than the A_{2u} modes. We expect that this splitting will be reduced or eliminated by screening due to the free carriers in the Cu-O planes.

B. Comparison with the measured Raman modes

As stated in the Introduction we used the measured Raman frequencies only for 2:1:2:2:8 to determine the Tl-O interaction parameters. These parameters mainly affect the highest [O(3) vibration] and the lowest three Raman A_{1g} modes of 2:1:2:2:8. Thus, except for these four modes, all the remaining modes listed in Table II are predictions of our model.

A comparison of the calculated Raman A_{1g} modes of 2:0:2:1:6 with the measurements (in parentheses) of Krantz et al.[13] shows that our calculations agree very well with the experimental data. A similar agreement is also seen for 1:1:2:2:7 where the experimental data are taken from Ref. 14. Note that for 1:1:2:2:7, the calculated A_{1g} mode at 358 cm^{-1} has no experimental counterpart. However, in the Raman spectrum of 1:1:2:2:7, McCarty[15] has observed a structure between 300 and 400 cm^{-1} and has attributed it to first-order Raman scattering. This observation is consistent with our calculation of the 358-cm^{-1} mode. For completeness we point out that in Ref. 14 McCarty et al. also report the observation of a shoulder at 465 cm^{-1} for which there is no counterpart in our calculations. However, McCarty[15] now believes that this shoulder is not due to first-order Raman scattering. The comparison of our calculations with the Raman data[16,17] for 2:1:2:2:8 has already been discussed in Ref. 1. Hence we do not repeat it here. For 1:2:2:3:9

and 2:2:2:3:10 the experimental Raman data are taken from Ref. 17. So far there are no Raman data available for 1:3:2:4:11. Also, there is no experimental counterpart to the mode calculated at 449 cm^{-1} in 1:2:2:3:9. However, all the remaining modes in 1:2:2:3:9 and 2:2:2:3:10 can be seen to be in good agreement with the measurements. Note that both the largest and the smallest deviations from the experimental data (in Table II) occur for 2:2:2:3:10: 420 (498) cm^{-1} (15.7% error) and 608 (601) cm^{-1} (1.2% error). The average deviation in Table II is found to be 7.7%. This quantitative agreement of our calculations with the Raman data supports our model which is based on a consistent set of interaction potentials for all the high-T_c materials we have investigated so far.

IV. SUMMARY AND CONCLUSIONS

In this paper we present a calculation of the optical modes of the thallium-based high-T_c superconductors, in the framework of a lattice dynamical model employing a common set of short-range interaction potentials which apply to the entire series of compounds and fits in with our earlier work on $YBa_2Cu_3O_7$ (Ref. 2) and $Bi_2CaSr_2Cu_2O_8$.[3] The model reproduces the available experimental infrared and Raman data of all these compounds quite well, and in doing so it is now supported by a rather broad database, albeit only of optical modes.

It is clear that questions about the underlying mechanism of the high-T_c superconductivity are beyond the scope of these calculations. Nevertheless our model cal-culations can contribute to this discussion in that it enables us to calculate the phonon dispersion curves of the "normal" compounds. Characteristic deviations from the normal behavior (phonon anomalies), revealed by inelastic neutron scattering experiments could then be interpreted as resulting from mechanisms which might be associated with the superconductivity. Such anomalous features could, for instance, be a characteristic softening of some phonons in a restricted region of wave-vector space, due to strong electron-phonon-coupling matrix elements.

At the present time we are calculating the complete phonon data for these compounds over the entire Brillouin zone. Thus, in addition to the phonon dispersion curves and the phonon density of states, we will be able to evaluate all phonon-related properties, such as mean-square amplitudes of vibration (thermal ellipses) and Debye-Waller factors, as well as the lattice specific heat (Debye temperature). The latter is of particular importance for a careful extraction of specific heat anomalies from experimental specific heat data.[18] Since many of these anomalies appear to be rather subtle, the subtraction of a simple Debye lattice specific heat may not be accurate enough to reveal the fine details of the anomalies.

[1] A. D. Kulkarni, J. Prade, F. W. de Wette, W. Kress, and U. Schröder, Phys. Rev. B **40**, 2642 (1989).

[2] W. Kress, U. Schröder, J. Prade, A. D. Kulkarni, and F. W. de Wette, Phys. Rev. B **38**, 2906 (1988).

[3] J. Prade, A. D. Kulkarni, F. W. de Wette, U. Schröder, and W. Kress, Phys. Rev. B **39**, 2771 (1989).

[4] J. Prade, A. D. Kulkarni, F. W. de Wette, W. Kress, M. Cardona, R. Reiger, and U. Schröder, Solid State Commun. **64**, 1267 (1987).

[5] In addition to stable phonon dynamics (dynamic stability), the crystal structure should also satisfy static stability criteria, namely, the equilibrium conditions of minimum potential energy and of vanishing forces on the ions. We are presently formulating these conditions. Requiring fulfillment of these equilibrium conditions will probably alter the short-range potentials and charges used in our model to some extent. However, the qualitative nature of the results presented here will remain unchanged.

[6] Y. Shimakawa, Y. Kubo, T. Manako, Y. Nakabayashi, and H. Igarashi, Physica C **156**, 97 (1988).

[7] B. Morosin, D. S. Ginley, P. F. Hlava, M. J. Carr, R. J. Baughman, J. E. Schirber, E. L. Venturini, and J. F. Kwak, Physica C **152**, 413 (1988).

[8] B. Morosin, D. S. Ginley, J. E. Schirber, and E. L. Venturini, Physica C **156**, 587 (1988).

[9] H. Ihara, R. Sugise, K. Hayashi, N. Terada, M. Jo, M.. Hirabayashi, A. Negishi, N. Atoda, H. Oyanagi, T. Shimomura, and S. Ohashi, Phys. Rev. B **38**, 11952 (1988).

[10] A. D. Kulkarni, F. W. de Wette, J. Prade, U. Schröder, and W. Kress, in *Proceedings of the Third International Conference on Phonon Physics (Phonons 89)*, edited by S. Hunklinger, W. Ludwig, and G. Weiss (World Scientific, Singapore, 1990).

[11] R. M. Macfarlane, H. Rosen, and H. Seki, Solid State Commun. **63**, 831 (1987).

[12] T. Zetterer, W. Ose, J. Schützmann, H. H. Otto, P. E. Obermayer, N. Tasler, H. Lengfellner, G. Lugert, J. Keller, and K. F. Renk, J. Opt. Soc. Am. B **6**, 420 (1989).

[13] M. Krantz, H. J. Rosen, R. M. Macfarlane, and V. Y. Lee, Phys. Rev. B **38**, 11962 (1988).

[14] K. F. McCarty, D. S. Ginley, D. R. Boehme, R. J. Baughman, E. L. Venturini, and B. Morosin, Physica C **156**, 119 (1988).

[15] K. F. McCarty (private communication).

[16] K. F. McCarty, D. S. Ginley, D. R. Boehme, R. J. Baughman, and B. Morosin, Solid State Commun. **68**, 77 (1988).

[17] K. F. McCarty, B. Morosin, D. S. Ginley, and D. R. Boehme, Physica C **157**, 135 (1989).

[18] S. E. Stupp and D. M. Ginsberg, Physica C **158**, 299 (1989).